1 **Supplementary Materials and Methods**

2 **Cell lines.**

3 THP-1 cells were obtained from the China National Collection of Authenticated Cell
4 Cultures and cultured in RPMI-1640 (Gibco, USA) with 10% fetal bovine serum (FBS)
5 (Gibco); Kasumi-1 and HL-60 cells were obtained from the National Collection of
6 Authenticated Cell Cultures and cultured in IMDM (Gibco) with 20% FBS; HL-
7 60/ADR cells were obtained from the Institute of Hematology & Blood Diseases
8 Hospital, Chinese Academy of Medical Science & Peking Union Medical College and
9 kept in RPMI-1640 with 10% FBS and IMDM with 10% FBS; HEK293T cells were
10 obtained from the China National Collection of Authenticated Cell Cultures and grown
11 in DMEM (Gibco) with 10% FBS. These cell lines are not among the commonly
12 misidentified cell lines and were authenticated by short tandem repeat (STR) analysis**.**

13

14 **Lentivirus infection**.

15 All the lentiviruses in this paper were packaged by GeneChem, Co., dCas9-VP46-Puro,
16 GV419-sgRNA-Neo, GV358-3FLAG-EGFP-Puro and CV186-3FLAG-mCherry-Puro
17 vectors were used. For lentivirus infection, METTL3 (GeneChem, China, SHCLNV:
18 NM_019852, Gene ID:56639) concentrated virus was directly added to cells. The
19 positively infected cells were selected with 1 μg/mL puromycin (Sigma-Aldrich,
20 #P8833).

21

22 For generation of dCas9 stable cell lines, cells were transduced with dCas9-VP64-Puro
23 lentivirus and then replaced with 2 mL of complete media containing puromycin. The
24 stably screened cells were transfected with sgMETTL3-GV419-Neo (GeneChem,
25 SHCLNV: NM_019852, Gene ID:56639) and its negative control lentivirus for

secondary transfection and then treated with G418 (Gibco, #10131) screening treatment. For the generation of single clones of THP-1-dCas9-sgMETTL3 and Kasumi-1-dCas9-sgMETTL3 cells, single cells were seeded in 96-well plates, and cells grown up from one single cell were selected.

RPPA.

Reverse Phase Protein Array (RPPA) was developed on THP-1 and THP-1/IDA cells by Mills Institute for Personalized Cancer Care, Fynn Biotechnologies Ltd.

Mouse studies and animal housing.

C57BL/6 or NSG mice were purchased from Beijing Vital River Laboratory Animal Technology Co., Ltd. All the animal experiments were carried out in accordance with the guidelines published by the Institutional Animal Care and Use Committee of Shandong University. All the animals were housed in an SPF animal house in the animal center of Qilu Hospital, Shandong University. MLL-AF9 secondary mouse leukemia cells were donated by the Institute of Hematology, Chinese Academy of Medical Sciences.

For the in vivo experiments shown in Fig. 3 and Supplementary Fig. S4, six- to eight-week-old male NSG mice were injected via the tail vein with three types of THP-1 cells (5×10^6 cells per mouse) that were transfected with viruses (THP-1-NC&-METTL3&-METTL3-CD cells). The treatment group was intraperitoneally treated with IDA (0.3 mg/kg per day for 7 days) beginning on day 42 after cell injection, and the control group was injected with PBS. An *in vivo* imaging system was used to quantitate disease burden by detecting up the GFP fluorescence signal. For the in vivo experiments shown

51 in Supplementary Fig. S5, six- to eight-week-old male C57BL/6 mice were injected by
52 the tail vein with three different kinds of MLL-AF9 cells (5×10^6 cells per mouse)
53 transfected with viruses. The treatment group was intraperitoneally treated with a daily
54 dose of 50 mg/kg Ara-C for 5 days along with a daily dose of 1.5 mg/kg DOX during
55 the first 3 days beginning on day 8 after cell injection. 1×10^5 BM cells and spleen cells
56 were harvested and analyzed the percentage of GFP- or mCherry- positive cells was
57 analyzed by flow cytometric analyses. Another batch of mice treated in the same way
58 was used for survival analysis.
59
60 For the homing and engraftment experiments shown in Fig. 4 and Supplementary Fig.
61 S7, three types of THP-1or MLL-AF9 cells that were transfected with viruses (-NC&-
62 METTL3&-METTL3-CD cells) were injected into NSG or C57BL/6 mice via tail-vein
63 injection (1×10^7 cells per mouse for homing analysis and 5×10^6 cells per mouse for
64 engraftment). Sixteen hours after BM transplantation for homing experiments and 1
65 week after MLL-AF9 transplantation or 6 weeks after THP-1 transplantation for
66 engraftment experiments, 1×10^5 BM cells and spleen cells were harvested and analyzed
67 the percentage of GFP- or mCherry- positive cells was analyzed by flow cytometric
68 analyses.
69
70 For the *in vivo* experiments shown in Fig. 5 and Supplementary Fig. S8, THP-1 cells
71 and THP-1/IDA cells were treated with DMSO or STM2457 (MedChemExpress,
72 Monmouth Junction, NJ, USA, #HY-134836, 20 μM), respectively, for 48 h before tail
73 vein injection. Sixteen hours after transplantation for homing experiments and 6 weeks
74 after transplantation for engraftment experiments. A total of 1×10^5 BM cells and spleen
75 cells were obtained and stained with anti-hCD45-APC (BioLegend, San Diego, CA,

76 USA, #304012), followed by flow cytometry.

77

78 To establish mouse models of primary AML patients, we injected the cryopreserved
79 leukemic blasts into NSG mice via tail-vein injection (2×10^6 cells per mouse, 2 mice
80 per patient). The percentage of CD45+ cells in the bone marrow and spleen of
81 euthanized animals was used to determine the extent of leukemia infiltration. The bone
82 marrow cells were extracted from femurs and tibia by crushing the bone in medium,
83 supplemented with 10% fetal bovine serum. To determine the response to
84 chemotherapeutic drugs, the mice were intraperitoneally injected with either IDA (0.3
85 mg/kg per day for 7 days) or PBS by beginning on day 35. The IDA response was
86 determined by flow cytometric analysis of CD45+ cells among the leukocytes isolated
87 from the bone marrow and spleen of mice in the PBS- and IDA-treated groups. All the
88 flow cytometric analyses were performed in Galias (Beckman Counter, Brea, Calif,
89 USA), and all data were analyzed by using FlowJo 10.4.

90

91 **EdU and CFA**.

92 For EdU assays, an iClick™ EdU Andy Fluor™ 647 Flow Cytometry Assay Kit (ABP
93 Biosciences, Rockville, MD, USA, #A008) was used, and the treated cells were tested
94 by flow cytometry. Cells from different groups were seeded in 6-well plates at a
95 concentration of 5×10^5 cells per well with PBS or IDA (0.005 μg/mL) for 24 h. For the
96 TR-14035 rescue experiment, cells from different groups and treated with 10 μM TR-
97 14035 (MedChemExpress, #HY-15770) or vehicle control DMSO combined with IDA
98 (0.005 μg/mL) for 24 hours prior to EdU experiments. All data were analyzed by using
99 Kaluza. For the colony-forming assay, treated cells were plated in methylcellulose
100 medium (MethoCult™ H4230, Stem Cell Technologies, Canada, #04230) according to

101 the manufacturer's instructions. Colonies were evaluated and scored after 14–21 days
102 of incubation.
103
104 **Cell migration and adhesion experiments.**
105 An 8 μm pore size Costar Transwell plate (Corning, NY, USA) was used to measure the
106 migratory potential of AML cells. A total of 4×10^5 cells were washed and resuspended.
107 For the TR-14035 rescue experiment, cells were suspended in 100 μL of RPMI-1640
108 medium containing 10 μM TR-14035 (MedChemExpress, #HY-15770) or vehicle
109 control DMSO and seeded in the upper chamber. For the STM2457 rescue experiment
110 in Fig. 5 and Supplementary Fig. S8, cells treated with 10 μM STM2457
111 (MedChemExpress, #HY-134836) or DMSO for 48h were suspended in 100 μL of
112 RPMI-1640 medium and seeded in the upper chamber. Next, 500 μL of RPMI-1640
113 medium containing 10% FBS was added to the lower well with HUVECs. After
114 incubation for 24 h, the migrated cells were measured by fluorescence microscopy and
115 analyzed. For the detection of cell adhesion, a total of 1×10^5 AML cells were seeded in
116 6-well plates covered with HUVECs. After incubation for 4 h, the adhered cells were
117 measured by fluorescence microscopy and analyzed.
118
119 **RT-PCR.**
120 Total RNA was extracted using TRIzol reagent (Thermo Fisher, #15596026) according
121 to the manufacturer's protocol and was reverse-transcribed into cDNA using
122 PrimeScript™ RT Master Mix (Takara, Japan, #RR036A). Quantitative real-time PCR
123 was performed using TB Green Premix Ex Taq™ II (Takara, #RR820A) on a Light
124 Cycler 480 II (Roche). GAPDH was used as endogenous control. The primer
125 sequences were: GAPDH, AAG GTG AAG GTC GGA GTC AAC and GGG GTC ATT

126 GAT GGC AAC AAT A; METTL3, CGT ACT ACA GGA TGA TGG CTT TC and TTT
127 CAT CTA CCC GTT CAT ACC C; ITGA4, CCA TCG TGA CTT GTG GGC A and
128 GTA AAT CAG GGG GCA CTC CA; 18 S, GTA ACC CGT TGA ACC CCA TT and
129 CCA TCC AAT CGG TAG TAG CG. The primer sequences for MeRIP qPCR were as
130 follows: Primer 1, AAC AGA AGA GAC AGT TGG AGT T and TCA TGA GTA AAA
131 GAA GTC CAA ACA A; Primer 2, CAT GCA AGG GGA AAA TCT CAG C and TAT
132 CTT CAA GGG CTT ACT TTT CTT G; Primer 3, GGG CTG TGT TCC AAC AAC
133 CA and ACA GAA AGA AAG ATG GTG AAA TCC A.
134

135 **m^6A dot blot.**

136 mRNA of AML cell sample was enriched by a Dynabeads mRNA Purification Kit
137 (Invitrogen, #61006) from total RNA. mRNA samples in a volume of 2 μL were
138 denatured by heating at 72°C for 5 min followed by immediate chilling on ice to prevent
139 secondary structure remodeling of mRNA. Then, mRNA was loaded on the Amersham
140 Hybond™-N+ membrane (GE Healthcare, Chicago, Illinois, USA, #RPN303B) and
141 crosslinked to the membrane twice by UV in autocrosslink mode (1 200 microjoules
142 [x100]; 25–50 sec) using UVP Crosslinker Analytik-jena. One of the membranes was
143 blocked with 5% nonfat powered milk (Sangon Biotech) in TBST and detected with an
144 m^6A-specific antibody (Synaptic Systems, Germany, #202003). The other membrane
145 was stained with methylene blue as a loading control.
146

147 **LC-MS/MS for determination of the m^6A/A ratio.**

148 Double selected polyadenylated (poly[A]) mRNA was digested by nuclease
149 phosphodiesterase I (0.1 U, Sigma), benzonase (10 U, Sigma) and alkaline phosphatase
150 (1 U, Sigma) in 50 μL of buffer containing 50 mM Tris-HCl, 1 mM $MgCl_2$ (pH = 8.0)

151 and 100 μg/mL BSA following incubation at 37°C for 3 h. The samples were diluted to
152 50 μL, filtered (0.22 mm pore size, 4 mm diameter, Millipore) and then loaded onto a
153 C18 reverse-phase column coupled online to an Agilent 6410 QQQ triple-quadrupole
154 LC mass spectrometer in positive electrospray ionization mode. The nucleosides were
155 quantified by using retention time and nucleoside to base ion mass transitions of 282.1–
156 150.1 (m^6A), 268–136 (A). Quantification was performed in comparison with the
157 standard curve obtained from pure nucleoside standards running with the same batch
158 of samples. The m^6A level was calculated as the ratio of m^6A to A.[1]

159

160 **RNA-seq and m^6A-seq.**

161 After 7 days of screening stably transfected cell with puromycin (1 μg/mL), THP-1-NC
162 and THP-1-METTL3 cells were harvested separately for the subsequent downstream
163 analysis of METTL3. Total RNA was extracted using TRIzol reagent (Thermo Fisher)
164 following the manufacturer's instructions, and the RIN number was determined to
165 evaluate the RNA integrity by an Agilent Bioanalyzer 2100 (Agilent Technologies).
166 Qualified total RNA was further purified by an RNAClean XP Kit (Beckman Coulter)
167 and RNase-Free DNase Set (QIAGEN).

168

169 For RNA-seq, a VAHTS Universal V6 RNA-seq Library Prep Kit for Illumina®
170 (Vazyme, #NR604-01) was used to establish the library. Each group was sequenced
171 with an Illumina HiSeq 2000, and the single-end sequencing length was 200-300 bp.
172 Sequence reads were compared with version 38 of the human genome (GRCH38) using
173 a standard Illumina sequence analysis pipeline.

174

175 For m^6A-seq, total RNA was fragmented into 100-200 nt RNA fragments using $ZnCl_2$

176 and incubated with anti-N6-Methyladenosine (m^6A) antibody (Sigma Aldrich,
177 #SAB5600251) Then, the products above were mixed with protein A/G magnetic beads
178 (Thermo Fisher, #88803) at 4 ℃. A NEBNext Ultra RNA library prep kit (NEB, #E7775)
179 was used to establish the library for the purified mRNA fragments. Each group was
180 sequenced with an Illumina NovaSeq 6000 sequencer, and the single-end sequencing
181 length was 150 bp. Reads were compared with human genome version GRCH38
182 through TopHat. ExomePeak ($P < 0.01$) was used to identify differential m^6A-modified
183 peaks between IP and input samples.
184

185 **RNA stability.**

186 Cells were treated with actinomycin D (Sigma-Aldrich, #A9415) at a final
187 concentration of 5 mg/mL for 0, 1, or 2 h/0, 1, 2, 3 or 4 h and collected. Cells were
188 harvested at the indicated time points, and total RNA was extracted and tested by qRT-
189 PCR. Relative mRNA levels were normalized to the starting point of treatment.
190

191 **Western blot.**

192 Cells were lysed in M-PER™ Mammalian Protein Extraction Reagent (Thermo Fisher,
193 #78501) with protease inhibitor cocktail (Roche). The membranes were incubated
194 sequentially with the diluted (1:1 000 or 1:500) primary and secondary antibodies. The
195 following antibodies were used to perform: METTL3/MT-A70 antibody (Bethyl,
196 Waltham, MA, USA, #A301-568A), Integrin Alpha 4 (Cell Signaling Technology,
197 #8440), beta Tubulin Antibody (Thermo Fisher, # 480011).
198

199 **Dual-luciferase reporter assays.**

200 The ITGA4–3'UTR containing the WT m^6A motifs and mutant motifs (m^6A was

201 replaced by T, see Supplementary Fig. S10E) was synthesized by Integrated DNA
202 Technologies and subcloned into the HindIII-SacI site of the pMIR-REPORT^{TM} firefly
203 luciferase reporter vector (Ambion, #GN1399). For dual-luciferase reporter assays, 400
204 ng WT or mutant firefly luciferase reporters (e.g., ITGA4-WT, ITGA4-mut), 500 ng
205 METTL3 expression vectors (e.g., METTL3-WT-pcDNA3, METTL3-CD-pcDNA3, or
206 pcDNA3), and 100 ng pRL-TK Renilla luciferase reporter vector (Promega, USA) were
207 cotransfected into HEK293T cells in 24-well plates using Lipofectamine 2000
208 (Invitrogen). The luciferase activities were assessed 48 h posttransfection by the Dual-
209 Luciferase Reporter Assay System (Promega, #E2920) and analyzed.
210
211 **Statistics.**
212 Sample size was chosen $n \geqslant 3$. Data were analyzed and presented as the mean ± SD.
213 Unpaired t test and correlativity test were used to analyze the two groups as indicated;
214 two-way ANOVA was used to compare the inter- and intra- differences of two factors
215 in two groups as indicated; $P < 0.05$ was considered significant. Statistical analyses
216 were performed using GraphPad Prism 9.0 or the R statistical environment. For Fig. 3C
217 and Supplementary Fig. S5G, Kaplan-Meier survival curves were generated using
218 GraphPad Prism 6, and the P values were calculated using the log rank test.

219 **Supplementary Figures and Figure Legends**

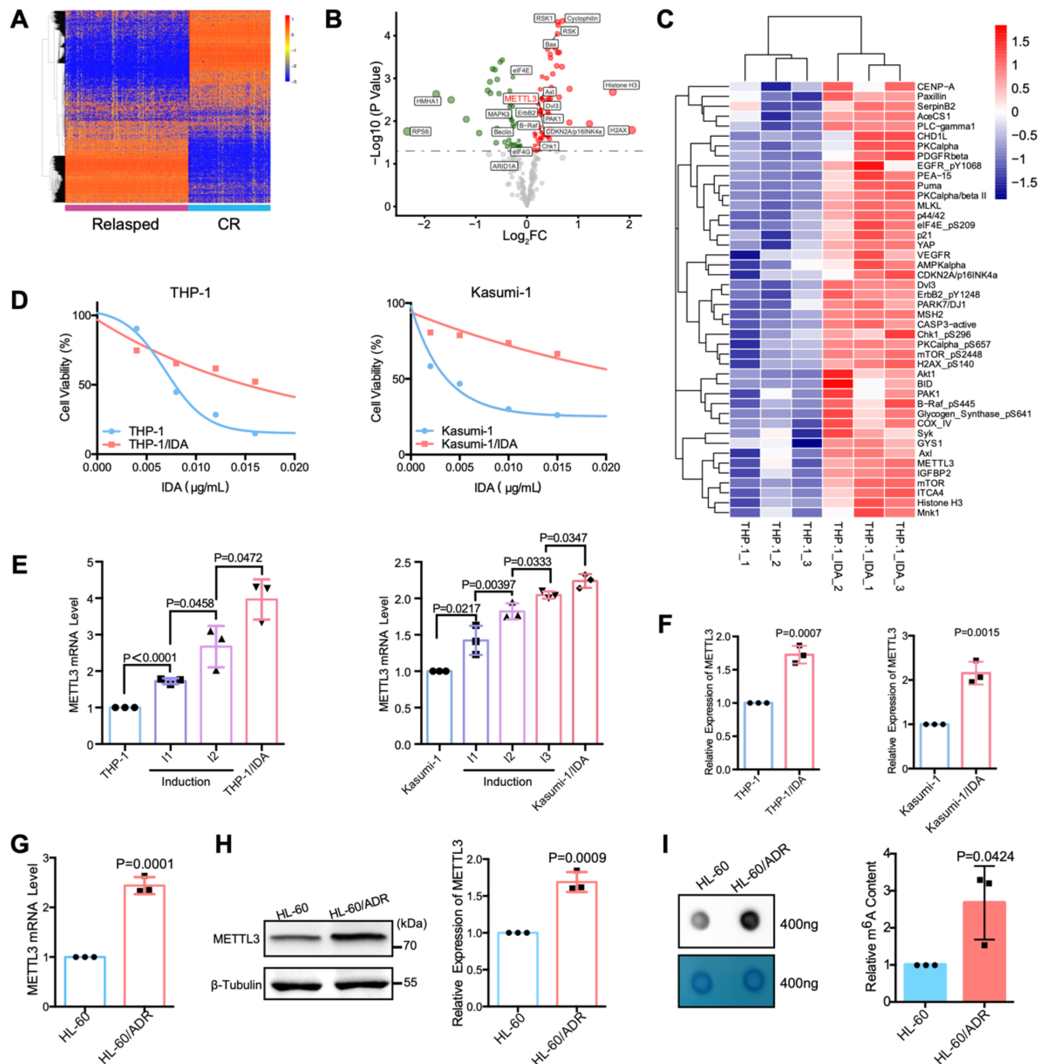

220

221 **Fig. S1 Screening process of METTL3 and its expression in chemotherapy-**
222 **resistant cell lines. A** Heatmaps showing the upregulated and downregulated genes
223 from GES165430 (n=268). **B** Volcano plot depicting proteins enriched in THP-1/IDA
224 cells (red) and THP-1 cells (green) analyzed by RPPA ($P < 0.05$). **C** Heatmaps showing
225 perturbed protein expression with significant increase in chemotherapy resistant cells
226 by RPPA (LogFC > 0.25). **D** CCK-8 assays of THP-1&THP-1/IDA cells and Kasumi-
227 1&Kasumi-1/IDA cells treated with IDA for 48 h (n=3). **E** qRT-PCR analysis showing
228 METTL3 expression at different induction periods in the chemotherapy-resistant cell
229 lines THP-1 and Kasumi-1. n=3, $P < 0.05$ was considered significant, t test. **F** Statistical

230 results of Western blot analysis for the expression of METTL3 in THP-1&THP-1/IDA

231 cells and Kasumi-1&Kasumi-1/IDA cells (*n*=3). **G** qRT-PCR analysis of METTL3

232 expression in HL-60/ADR cells (*n*=3). **H** Western blot analysis for the expression of

233 METTL3 in HL-60/ADR cells and the statistical results (*n*=3). **I** HL-60&HL-60/ADR

234 cells were subjected to mRNA extraction followed by m^6A dot blot assays to detect

235 global m^6A changes and summarized. *n*=3, MB, methylene blue staining (as loading

236 control). Mean ± SD values are shown for (**E**)-(**I**). $P < 0.05$ was considered significant;

237 t test.

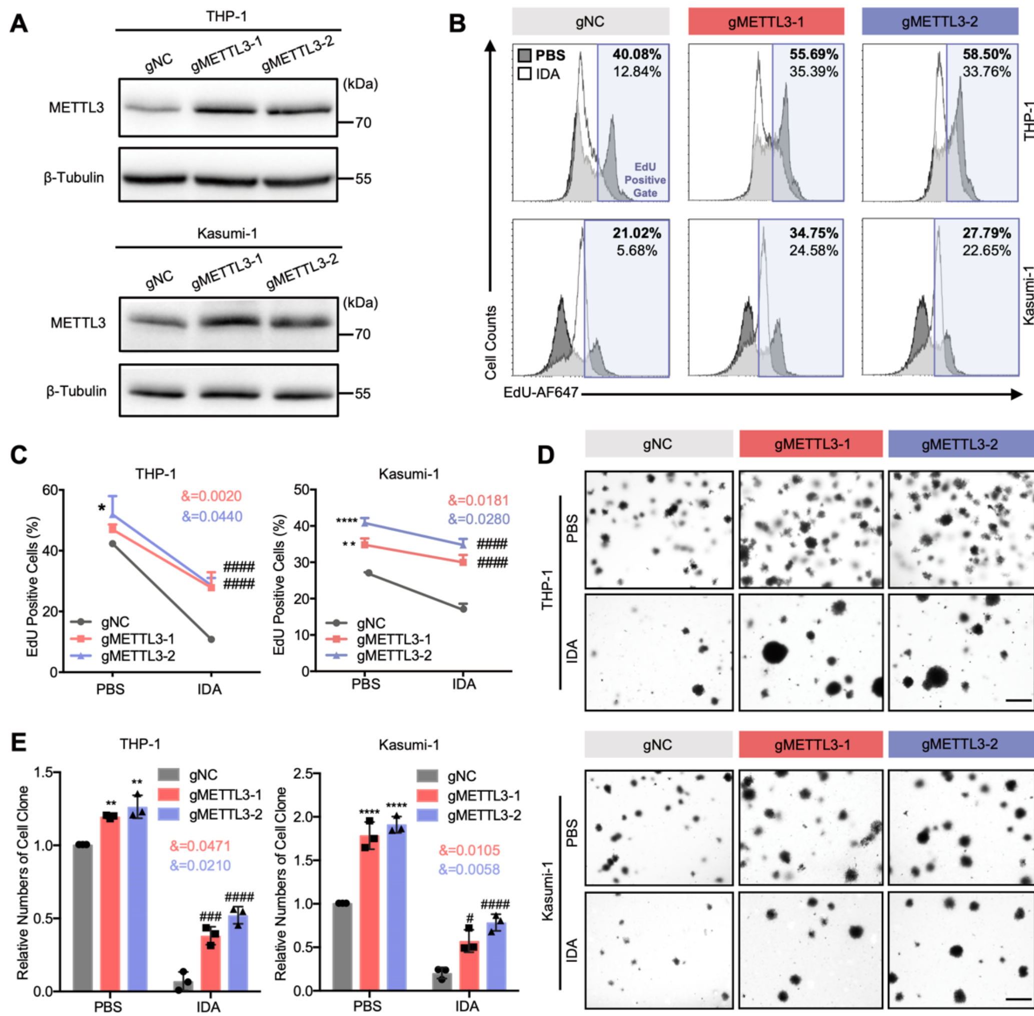

238

239 **Fig. S2 The overexpression of endogenous METTL3 confers chemoresistance to**

240 **AML cells. A-C** The overexpression efficiency was confirmed by Western blot and

241 shown in (**A**). EdU incorporation assay showing the percentage of AML cells (n=3)

242 entering the proliferation cycle (EdU positive cells) with or without IDA pressure (**B**)

243 and are summarized (**C**). **D-E** Colony-forming assay (**D**) showing images of AML cells

244 with or without IDA pressure. Bar, 500 μm. Statistical analysis is shown in (**E**). Mean

245 ± SD values are shown for (**C**) and (**E**). *, $P < 0.05$, **, $P < 0.01$, ****, $P < 0.0001$, vs.

246 the NC group with PBS treatment; $^{\#}$, $P < 0.05$, $^{\#\#\#}$, $P < 0.001$, $^{\#\#\#\#}$, $P < 0.0001$, vs. the

247 NC group with IDA treatment; &, significant interaction effect; two-way ANOVA.

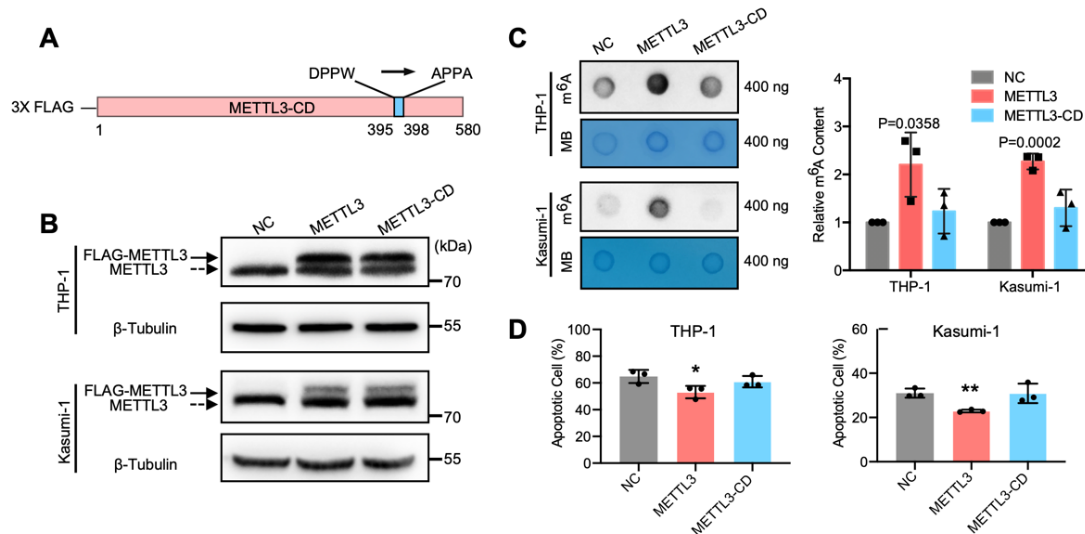

248

249 **Fig. S3 The overexpression of exogenous METTL3/METTL3-CD and**
250 **corresponding mRNA m^{6}A modification confirmation. A** Construction of METTL3-
251 CD vectors. **B-C** Western blot (**B**) confirmation and corresponding changes in the
252 mRNA m^{6}A expression levels (**C**) were measured by m^{6}A dot blot assays (left) and
253 summarized (right). Data are mean ± SD values. $P < 0.05$ was considered significant, t
254 test. **D** Percentage of apoptotic cells in a THP-1 and Kasumi-1 cells from three replicate
255 experiments. n=3, Mean ± SD values are shown for (**C**) and (**D**). *, $P < 0.05$, **, $P <$
256 0.01, t test.

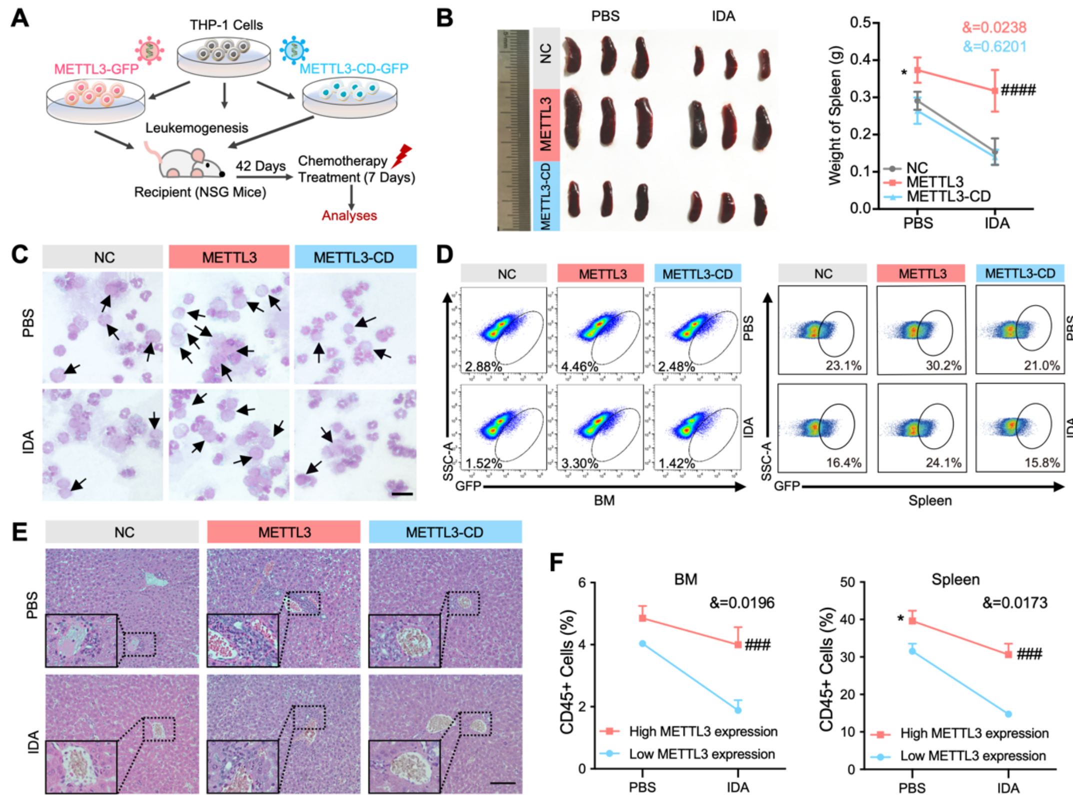

Fig. S4 METTL3 reduces the sensitivity of AML cells to chemotherapeutics in xenograft model. **A** Scheme of the design and procedures of the chemotherapy treatment sensitivity test with AML mice using NSG mice. **B** Spleen image and weight index from xenograft recipient mice with or without IDA treatment at the end point. *, $P < 0.05$, vs. the NC group with PBS treatment; $^{\#\#\#\#}$, $P < 0.0001$, vs. the NC group with IDA treatment; &, significant interaction effect; two-way ANOVA. **C**-**D** Wright-Giemsa staining of BM of the xenograft recipient mice at the end point is shown in (**C**); and the engraftment of THP-1 cells in BM and spleen of the NSG mice is shown in (**D**). Bar, 50 μm. **E** H&E staining of the liver of the xenograft recipient mice at the end point. Bar, 200 μm. **F** CD45+ cells infiltration in the high METTL3 expression group (n=3) and the low METTL3 expression group (n=3) of patient-derived xenografts (PDX models) with or without IDA treatment. Mean ± SD values are shown for (**B**) and (**F**).

270 *, $P < 0.05$, vs. the low METTL3 expression group with PBS treatment; [###], $P < 0.001$,

271 vs. the low METTL3 expression group with IDA treatment; &, significant interaction

272 effect; two-way ANOVA.

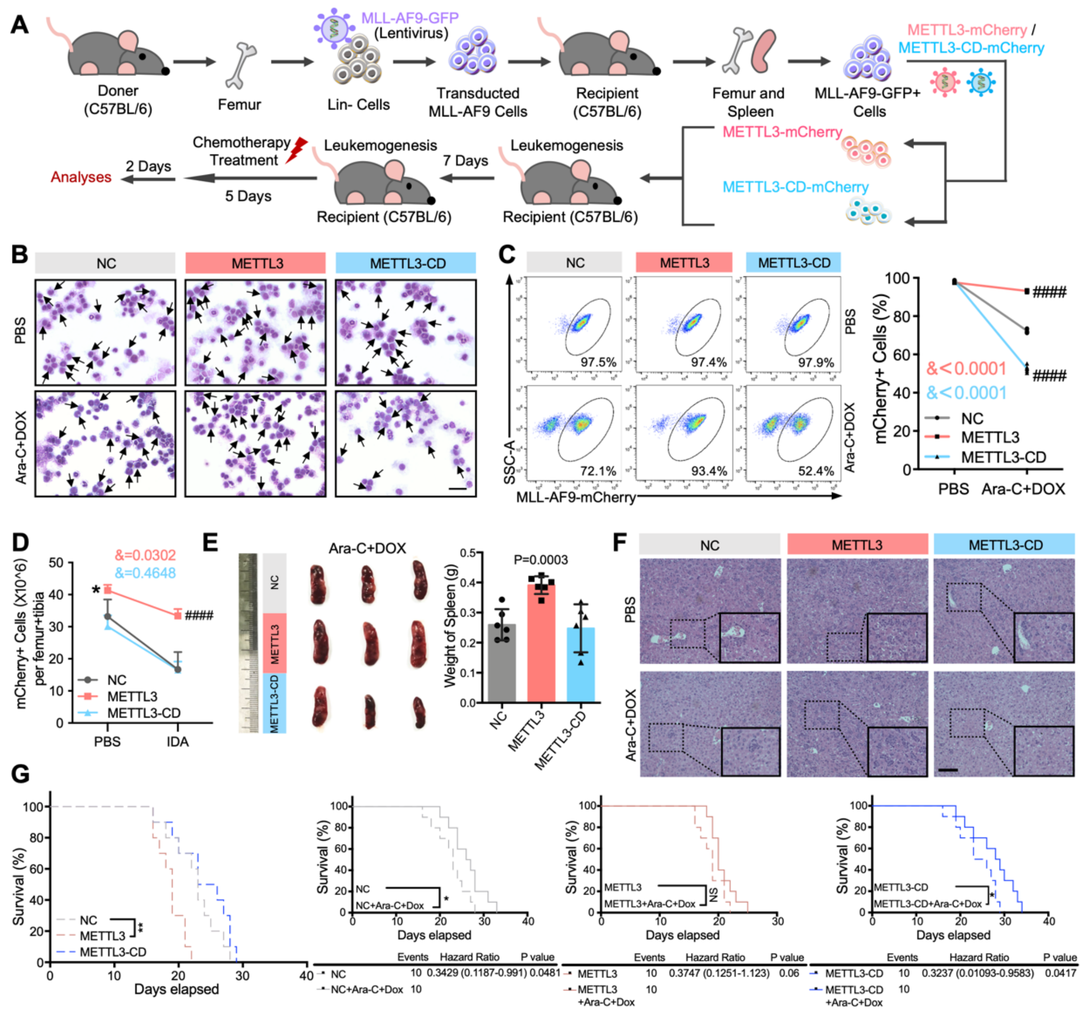

Fig. S5 METTL3-meditated m^{6}A reduces the sensitivity to chemotherapeutics of MLL-AF9+ AML mice. **A** Schematic outline of the experimental strategy of primary and secondary BMT using MLL-AF9 leukemic cells. **B** Wright-Giemsa staining of BM of the BMT recipient mice with or without Ara-C and DOX treatment on the 14th day. **C** and engraftment of MLL-AF9 cells in BM of the BMT recipient mice with or without chemotherapy treatment is shown and summarized. Bar, 50 μm. $^{\#\#\#\#}$, $P < 0.0001$, vs. the NC group with PBS treatment; &, significant interaction effect; two-way ANOVA. **D** Absolute counts of MLL-AF9 cell infiltration in the BM of BMT recipient mice with or without chemotherapy. *, $P < 0.05$, vs. the NC group with PBS treatment; $^{\#\#\#\#}$, $P <$ 0.0001, vs. the NC group with IDA treatment; &, significant interaction effect; two-

284 way ANOVA. **E** Spleen image and weight index of BMT recipient mice treated with
285 Ara-C and DOX at the end point. $P < 0.05$ was considered significant, t test. **F** H&E
286 staining of the livers of the BMT recipient mice at the end point. Bar, 200 μm. **G**
287 Kaplan-Meier survival curves showing the effects of forced METTL3 expression on
288 the progression of MLL-AF9 cells in BMT recipient mice. *, $P < 0.05$, **, $P < 0.01$;
289 NS, nonsignificant; t test. $n \geqslant 5$, mean ± SD values are shown for (**C**) and (**D**)-(**E**).

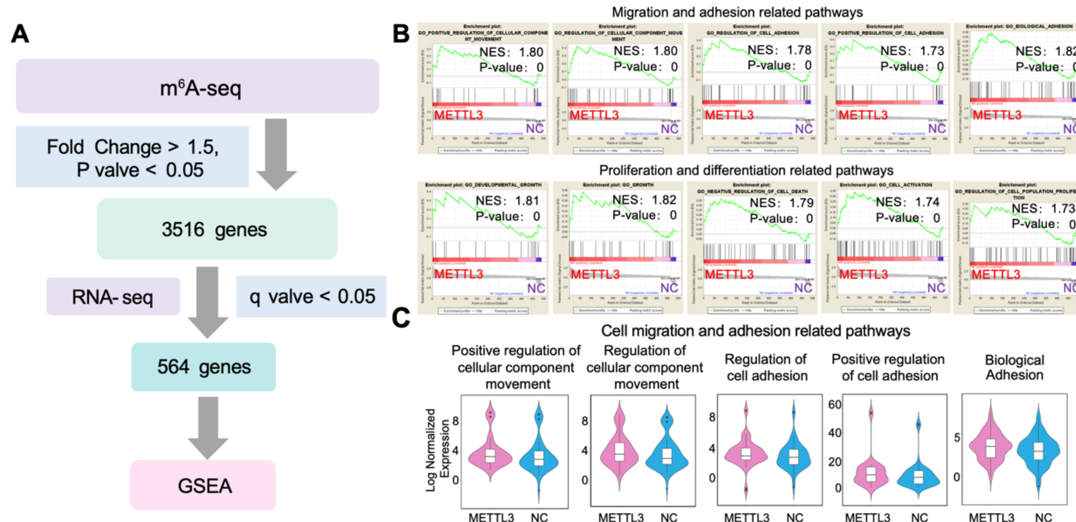

290

291 **Fig. S6 METTL3 downstream analysis and GSEA A** Schematic of METTL3
292 downstream analysis. **B** GSEA in THP-1 cells. Representative gene sets that were
293 significantly enriched in the METTL3 overexpression samples (left panel) or the
294 control samples (right panel) are shown. METTL3, METTL3 overexpression; NC,
295 control; NES, normalized enrichment score; FDR, false discovery rate. **C** Violin plots
296 showing the relative abundance of genes involved in the indicated migration/adhesion-
297 related pathways in METTL3-overexpressing or control THP-1 cells.

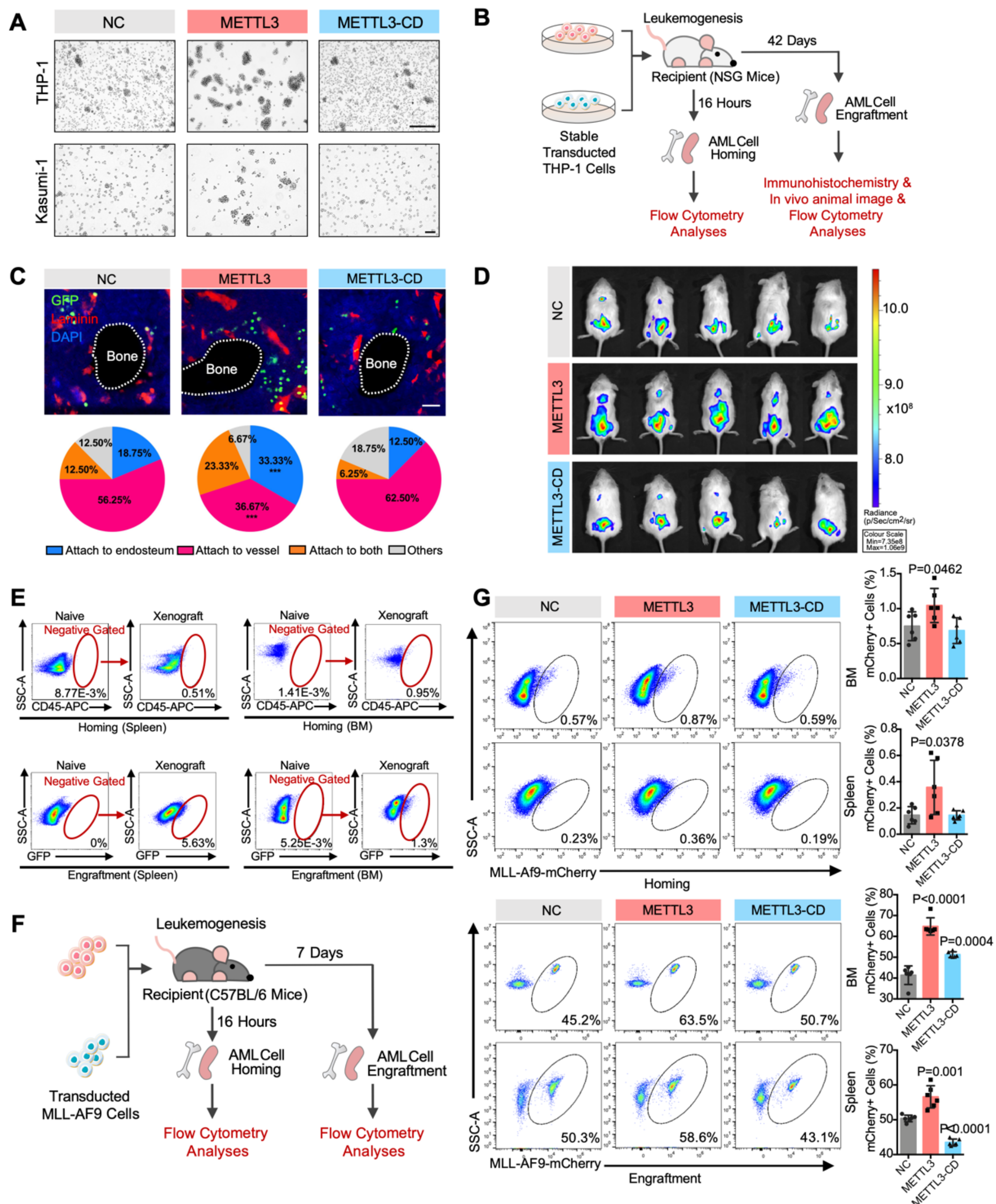

298

299 **Fig. S7 AML homing and engraftment in xenograft/homograft recipient mice. A**

300 Images showing that METTL3-overexpressing AML cells have clustered growth

301 characteristics. **B** Scheme of the design and procedures of the homing/engraftment test

302 in AML xenograft recipient mice. **C** Representative images of localizations of THP-1

303 cells (GFP) in the vasculature (laminin, red) of the recipients (top); percentages of THP-

304 1 cells attached to the endosteal niche, vascular niche, or both in (bottom). **D** *In vivo*

305 animal imaging was carried out on the xenograft mice 42 days after tail vein injection.

306 **E** The flow cytometry gate principle for homing and engraftment of THP-1 cells in the
307 spleen and bone marrow (BM) of NSG mice. **F** Scheme of the design and procedures
308 of the homing/engraftment test in AML homograft recipient mice. **G** Flow cytometry
309 was carried out for the homograft recipient mouse BM and spleen 16 h/7days after tail
310 vein injection. The statistical results are shown on the right. $P < 0.05$ was considered
311 significant vs. the NC group, t test. $n \geqslant 5$, mean ± SD values are shown for (**G**).

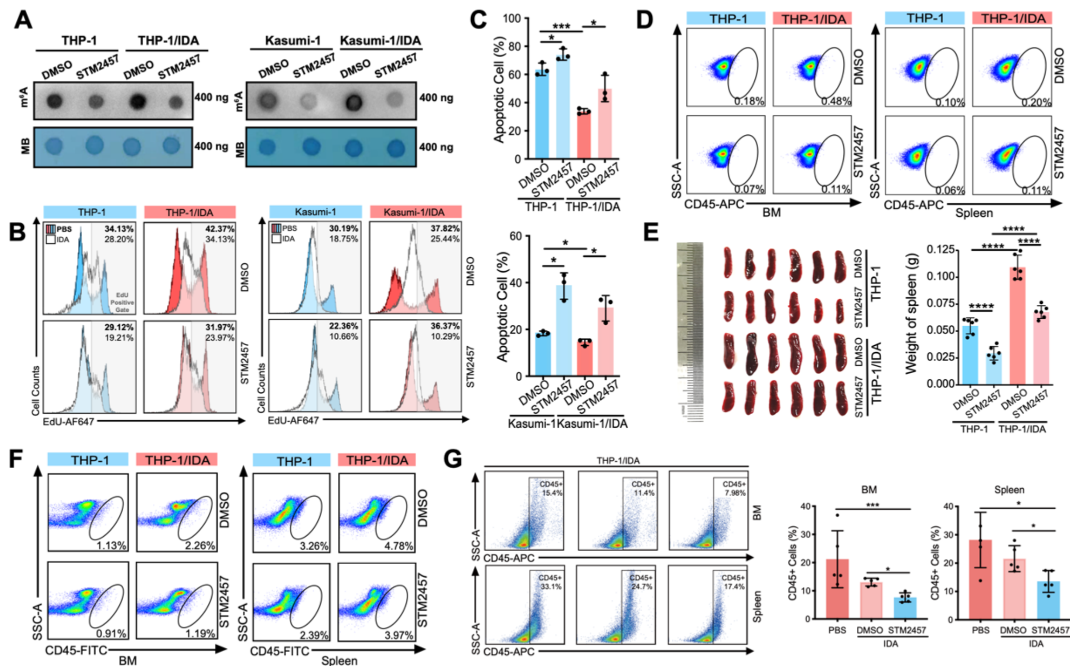

Fig. S8 A METTL3 inhibitor reverses AML chemoresistance and homing/engraftment capacity. A THP-1&THP-1/IDA and Kasumi-1&Kasumi-1/IDA cells with or without STM2457 treatment for 48 h were subjected to mRNA extraction followed by m^{6}A dot blot assays to detect global m^{6}A changes. MB, methylene blue staining (as loading control). **B** EdU incorporation assay showing the improvement of AML proliferation can be reversed by the pretreatment of STM2457 with or without IDA pressure. Percentages after PBS treatment are shown in bold, and percentages after IDA treatment are shown in regular. **C** The percentage of apoptotic cells showed that METTL3 inhibitor treatment promoted the apoptosis of AML cells (n=3). Data are mean ± SD values. *, P<0.05, ***, P<0.001, t test. **D** The homing of THP-1&THP-1/IDA cells with or without STM2457 pretreatment in the BM and spleen measured by flow cytometry 16 h after tail vein injection. **E** Spleen image (left) and weight index (right) from xenograft recipient mice (n=6) 42 days after tail vein injection. Data are mean ± SD values. ****, P < 0.0001; t test. **F** The engraftment of THP-1&THP-1/IDA cells with or without STM2457 pretreatment in the BM and spleen

328 measured by flow cytometry 42 days after tail vein injection. **G** STM2457 rescued the

329 sensitivity of THP-1/IDA cells (n=5) *in vivo*. Statistical analysis is shown in right. Data

330 are mean ± SD values. *, $P < 0.05$, ***, $P < 0.001$; t test.

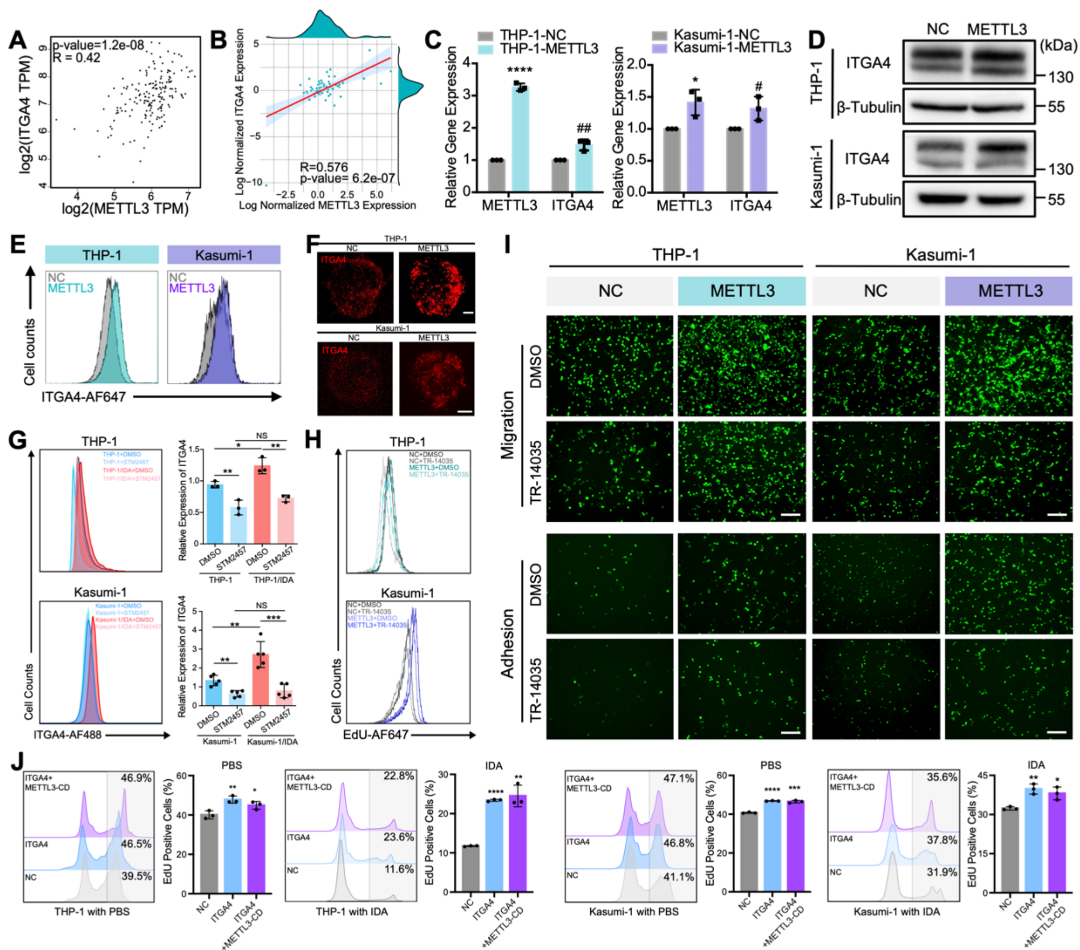

331

332 **Fig. S9 METTL3 mediates AML chemoresistance by regulating ITGA4. A-B** The

333 Pearson correlation of ITGA4 with METTL3 mRNA expression across the AML

334 samples in TCGA (**A**) and clinical data (**B**). $P < 0.05$ was considered significant. **C-F**

335 Changes in ITGA4 expression are shown by qPCR analysis (**C**), Western blot analysis

336 (**D**), flow cytometry (**E**), and immunofluorescence (**F**). Bar, 5 µm. *, $P < 0.05$, ****, P

337 < 0.0001, METTL3 expression vs. the NC group; $^{\#}$, $P < 0.05$, $^{\#\#}$, $P < 0.01$, ITGA4

338 expression vs. the NC group, t test. **G** Changes in ITGA4 expression with or without

339 STM2457 treated are shown by flow cytometry. Statistical analysis is shown on right.

340 *, $P < 0.05$, **, $P < 0.01$; ***, $P < 0.001$, NS, nonsignificant; t test. **H** EdU

341 incorporation assay showing that the improvement in the percentage of METTL3-

342 overexpressing AML cells entering the proliferation cycle with IDA pressure can be

343 partly reversed by TR-14035. **I** Images showing that the improvement of migration and

344 adhesion in METTL3-overexpressing AML cells can be partly reversed by TR-14035.

345 **J** EdU incorporation assay showing ITGA4 overexpression promoted AML

346 chemoresistance. *, $P < 0.05$, **, $P < 0.01$, ***, $P < 0.001$, ****, $P < 0.0001$; t test. n

347 $\geqslant 3$, mean ± SD values are shown for (**C**), (**G**) and (**J**).

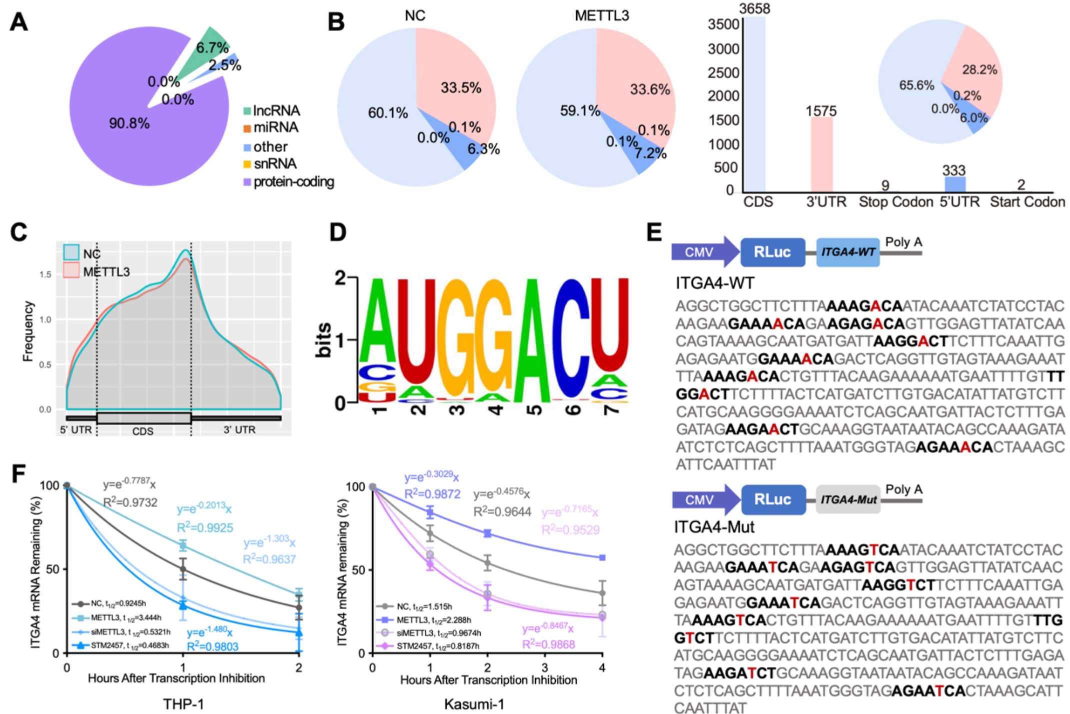

348

349 **Fig. S10 METTL3 regulates stability of ITGA4 mRNA. A** Pie charts showing the
350 distribution of m^{6}A-seq reads in RNA classes. **B** The distribution of total m^{6}A peaks in
351 the indicated regions of mRNA transcripts in the control and METTL3-overexpressing
352 cells. **C** The proportion of m^{6}A peak distribution in the 5' UTR, start codon, CDS, stop
353 codon or 3' UTR across the entire set of mRNA transcripts. **D** The predominant
354 consensus motif DRACH ([G/A/U] [G/A] m^{6}AC [U/A/C]) detected by HOMER in
355 m^{6}A-seq. **E** Construction of luciferase reporter vectors. The positions of the ITGA4
356 sequences used relative to their transcription start sites are shown. Putative m^{6}A
357 consensus sequences are in bold, while the mutation sites are in red. **F** The mRNA half-
358 life ($t_{1/2}$) of ITGA4 transcripts in THP-1 and Kasumi-1 cells with STM2457 inhibition
359 or METTL3 knockdown/overexpression THP-1 and Kasumi-1 cells.

360 **References**

361 1. Su D, Chan CT, Gu C, Lim KS, Chionh YH, McBee ME*, et al.* Quantitative
362 analysis of ribonucleoside modifications in tRNA by HPLC-coupled mass
363 spectrometry. *Nat Protoc* 2014 Apr; **9**(4)**:** 828-841.

364